Geochemical Perspectives Letters

Nucleosynthetic *s*-Process Depletion in Mo from Ryugu samples returned by Hayabusa2

N. Nakanishi[1,2,3*], T. Yokoyama[2], A. Ishikawa[2], R.J. Walker[1], Y. Abe[4], J. Aléon[5], C.M.O'D Alexander[6], S. Amari[7,8], Y. Amelin[9], K.-I. Bajo[10], M. Bizzarro[11], A. Bouvier[12], R.W. Carlson[6], M. Chaussidon[13], B.-G. Choi[14], N. Dauphas[15], A.M. Davis[15], T. Di Rocco[16], W. Fujiya[17], R. Fukai[18], I. Gautam[2], M.K. Haba[2], Y. Hibiya[19], H. Hidaka[20], H. Homma[21], P. Hoppe[22], G.R. Huss[23], K. Ichida[24], T. Iizuka[25], T.R. Ireland[26], S. Itoh[27], N. Kawasaki[10], N.T. Kita[28], K. Kitajima[28], T. Kleine[29], S. Komatani[24], A.N. Krot[23], M.-C. Liu[30], Y. Masuda[2], M. Morita[24], K. Motomura[31], F. Moynier[13], I. Nakai[32], K. Nagashima[23], A. Nguyen[33], L. Nittler[6], M. Onose[24], A. Pack[16], C. Park[34], L. Piani[35], L. Qin[36], S.S. Russell[37], N. Sakamoto[38], M. Schönbächler[39], L. Tafla[30], H. Tang[36], K. Terada[40], Y. Terada[41], T. Usui[18], S. Wada[10], M. Wadhwa[42], K. Yamashita[43], Q.-Z. Yin[44], S. Yoneda[45], E.D. Young[30], H. Yui[46], A.-C. Zhang[47], T. Nakamura[48], H. Naraoka[49], T. Noguchi[27], R. Okazaki[49], K. Sakamoto[18], H. Yabuta[50], M. Abe[18], A. Miyazaki[18], A. Nakato[18], M. Nishimura[18], T. Okada[18], T. Yada[18], K. Yogata[18], S. Nakazawa[18], T. Saiki[18], S. Tanaka[18], F. Terui[51], Y. Tsuda[18], S.-I. Watanabe[20], M. Yoshikawa[18], S. Tachibana[52], H. Yurimoto[10]

OPEN ACCESS

Abstract

https://doi.org/10.7185/geochemlet.2341

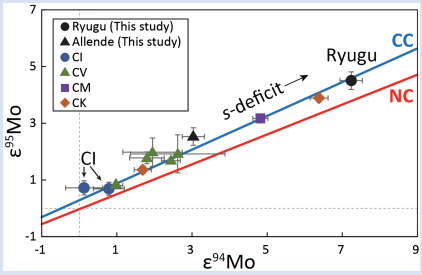

Initial analyses of samples collected from two locations on the asteroid Ryugu indicated that the mineralogical, chemical, and isotopic characteristics of the Ryugu samples show similarities to carbonaceous chondrites, particularly the Ivuna-type (CI) group. In this study, we analysed a composite sample of four bulk Ryugu samples (A0106, A0106-A0107, C0107, and C0108) collected from both sampling locations that were combined in order to determine its mass independent Mo isotopic composition and reveal contributions from diverse nucleosynthetic sources. The ε^{94}Mo and ε^{95}Mo values for the Ryugu sample are characterised by the carbonaceous chondrite (CC)-type, which is consistent with the nucleosynthetic isotope compositions observed for other elements (Cr, Ti, Fe, and Zn). The Ryugu composite sample, however, is characterised by greater *s*-process depletion of Mo isotopes compared with any known bulk carbonaceous chondrite, even including CI chondrites. The observed Mo isotopic signature in the Ryugu composite was most likely caused by either incomplete digestion of *s*-process-rich presolar SiC, or biased sampling of materials enriched in aqueously-formed secondary minerals characterised by *s*-process-poor Mo isotopes, resulting from the physicochemical separation between *s*-process-rich presolar grains and a complementary *s*-process-poor aqueous fluid in the Ryugu parent body.

Received 30 June 2023 | Accepted 15 November 2023 | Published 20 December 2023

Introduction

The Hayabusa2 mission by JAXA performed two sampling sequences on the asteroid (162173) Ryugu, and returned 5.4 g of the asteroid materials back to Earth (Tachibana *et al.*, 2022). Spectral observations led to the classification of the asteroid Ryugu as Cb-type, which has long been assumed to be related to carbonaceous chondrite meteorites (Bus and Binzel, 2002). This observation was confirmed by the initial analyses of returned samples; the mineralogical, chemical, and isotopic characteristics of the Ryugu samples showed similarities to carbonaceous chondrites, in particular the Ivuna-type (CI) group

1. Department of Geology, University of Maryland, College Park, MD 20742, USA
2. Department of Earth and Planetary Sciences, Tokyo Institute of Technology, Tokyo 152-8551, Japan
3. Department of Earth Sciences, Waseda University, Tokyo 169-8050, Japan
4. Graduate School of Engineering, Tokyo Denki University, Tokyo 120-8551, Japan
5. Institut de Minéralogie, de Physique des Matériaux et de Cosmochimie, Sorbonne Université, Museum National d'Histoire Naturelle, CNRS UMR 7590, IRD, 75005 Paris, France
* Corresponding author (email: nnakanishi@aoni.waseda.jp)

(Hopp *et al.*, 2022; Moynier *et al.*, 2022; Nakamura *et al.*, 2022, 2023; Paquet *et al.*, 2023; Yokoyama *et al.*, 2023a). Chemical and physical properties of the returned samples suggest that the parent asteroid of Ryugu was accreted in the outer Solar System where water and CO_2 were present as ices, followed by melting of the accreted ice due to the radioactive decay of ^{26}Al that heated the parent asteroid to ~40 °C (Nakamura *et al.*, 2023). The melting of the ice led to the hydration of the inner portion of the parent body, causing pervasive aqueous alteration that resulted in the precipitation of secondary minerals, including phyllosilicates, carbonates, oxides, sulfides, and phosphates (Nakamura *et al.*, 2022, 2023; Yokoyama *et al.*, 2023a).

Nucleosynthetic isotopic anomalies of meteorites provide robust information that can be used to constrain the origin of materials that contributed to the accretion of their parent bodies (Dauphas and Schauble, 2016; Yokoyama and Walker, 2016). Isotopic compositions of Cr, Ti, Fe, and Zn have been reported for Ryugu samples, all of which are generally consistent with those of CI chondrites (Hopp *et al.*, 2022; Paquet *et al.*, 2023; Yokoyama *et al.*, 2023a). These observations suggest that the parent bodies of Ryugu and CI chondrites formed in a common source reservoir in the outer Solar System. Remarkably, both Ryugu materials and CI chondrites show variable ε^{54}Cr values ($\varepsilon^{54}Cr = [(^{54}Cr/^{52}Cr)_{sample}/(^{54}Cr/^{52}Cr)_{standard} - 1] \times 10^4$; ranging from $+1.22 \pm 0.06$ to $+2.22 \pm 0.13$ for Ryugu and from $+0.84 \pm 0.14$ to $+1.94 \pm 0.12$ for CI chondrites), which exceed the range of analytical uncertainties (Kadlag *et al.*, 2019; Williams *et al.*, 2020; Nakamura *et al.*, 2022; Yokoyama *et al.*, 2023a, b). The isotopic heterogeneity was most likely caused by physicochemical fractionation between ^{54}Cr-rich presolar grains and Cr-bearing secondary minerals during aqueous alteration in the parent bodies (Yokoyama *et al.*, 2023b). By contrast, the mass independent isotopic compositions of Ti, Fe, and Zn of Ryugu samples are homogeneous, and are within the range of CI meteorite compositions. Given the contrast between Cr and other isotopic tracers, it is important to assess whether there are other elements characterised by isotopic heterogeneities in Ryugu materials, and between Ryugu samples and CI chondrites. The nature of any differences may provide important further insights to the causes of the heterogeneities.

Molybdenum is a moderately siderophile element with seven stable isotopes synthesised by a combination of the *s*-process (trace ^{94}Mo, ^{95}Mo, ^{96}Mo, ^{97}Mo, ^{98}Mo, and trace ^{100}Mo), the *r*-process (^{95}Mo, ^{97}Mo, ^{98}Mo, and ^{100}Mo), and the processes that produce proton-rich nuclides (^{92}Mo and ^{94}Mo). Thus, the mass independent isotopic compositions of Mo in meteorites vary in accordance with differences in the proportions of various nucleosynthetic components present in bulk meteorite samples. High precision measurements of Mo isotopes in bulk chondrites and differentiated meteorites have revealed considerable variation among early Solar System materials (*e.g.*, Dauphas *et al.*, 2002; Budde *et al.*, 2016; Spitzer *et al.*, 2020). In particular, an internal isotopic dichotomy of ε^{94}Mo-ε^{95}Mo ($\varepsilon^{i}Mo = [(^{i}Mo/^{96}Mo)_{sample}/(^{i}Mo/^{96}Mo)_{standard} - 1] \times 10^4$) between non-carbonaceous meteorites (NC) and carbonaceous meteorites (CC) has been shown to be particularly sensitive for evaluating genetic differences of source materials present in bulk meteorite samples (Budde *et al.*, 2016; Poole *et al.*, 2017; Worsham *et al.*, 2017). Additionally, the Mo isotope compositions of meteorites can be modified by parent body processes, including thermal metamorphism (Yokoyama *et al.*, 2019), and presumably

6. Earth and Planets Laboratory, Carnegie Institution for Science, Washington, DC, 20015, USA
7. McDonnell Center for the Space Sciences and Physics Department, Washington University, St. Louis, MO 63130, USA
8. Geochemical Research Center, The University of Tokyo, Tokyo, 113-0033, Japan
9. Korea Basic Science Institute, Ochang, Cheongwon, Cheongju, Chungbuk 28119, Republic of Korea
10. Department of Natural History Sciences, Hokkaido University, Sapporo 001-0021, Japan
11. Centre for Star and Planet Formation, GLOBE Institute, University of Copenhagen, Copenhagen, K 1350, Denmark
12. Bayerisches Geoinstitut, Universität Bayreuth, Bayreuth 95447, Germany
13. Université Paris Cité, Institut de physique du globe de Paris, CNRS, 75005 Paris, France
14. Department of Earth Science Education, Seoul National University, Seoul 08826, Republic of Korea
15. Department of the Geophysical Sciences and Enrico Fermi Institute, The University of Chicago, 5734 South Ellis Avenue, Chicago 60637, USA
16. Faculty of Geosciences and Geography, University of Göttingen, Göttingen, D-37077, Germany
17. Faculty of Science, Ibaraki University, Mito 310-8512, Japan
18. ISAS/JSEC, JAXA, Sagamihara 252-5210, Japan
19. Research Center for Advanced Science and Technology, The University of Tokyo, Tokyo 153-8904, Japan
20. Department of Earth and Planetary Sciences, Nagoya University, Nagoya 464-8601, Japan
21. Osaka Application Laboratory, SBUWDX, Rigaku Corporation, Osaka 569-1146, Japan
22. Max Planck Institute for Chemistry, Mainz 55128, Germany
23. Hawai'i Institute of Geophysics and Planetology, University of Hawai'i at Mānoa, Honolulu, HI 96822, USA
24. Analytical Technology, Horiba Techno Service Co., Ltd., Kyoto 601-8125, Japan
25. Department of Earth and Planetary Science, The University of Tokyo, Tokyo 113-0033, Japan
26. School of Earth and Environmental Sciences, The University of Queensland, St Lucia QLD 4072, Australia
27. Division of Earth and Planetary Sciences, Kyoto University, Kyoto 606-8502, Japan
28. Department of Geoscience, University of Wisconsin-Madison, Madison, WI 53706, USA
29. Max Planck Institute for Solar System Research, 37077 Göttingen, Germany
30. Department of Earth, Planetary, and Space Sciences, UCLA, Los Angeles, CA 90095, USA
31. Thermal Analysis, Rigaku Corporation, Tokyo 196-8666, Japan
32. Department of Applied Chemistry, Tokyo University of Science, Tokyo 162-8601, Japan
33. Astromaterials Research and Exploration Science, NASA Johnson Space Center, Houston, TX 77058, USA
34. Earth-System Sciences, Korea Polar Research Institute, Incheon 21990, Korea
35. Centre de Recherches Pétrographiques et Géochimiques, CNRS - Université de Lorraine, 54500 Nancy, France
36. CAS Key Laboratory of Crust-Mantle Materials and Environments, University of Science and Technology of China, School of Earth and Space Sciences, Anhui 230026, China
37. Department of Earth Sciences, Natural History Museum, London, SW7 5BD, UK
38. Isotope Imaging Laboratory, Creative Research Institution, Hokkaido University, Sapporo 001-0021, Japan
39. Institute for Geochemistry and Petrology, Department of Earth Sciences, ETH Zurich, 8092 Zurich, Switzerland
40. Department of Earth and Space Science, Osaka University, Osaka 560-0043, Japan
41. Spectroscopy and Imaging, Japan Synchrotron Radiation Research Institute, Hyogo 679-5198 Japan
42. School of Earth and Space Exploration, Arizona State University, Tempe, AZ 85281, USA
43. Graduate School of Natural Science and Technology, Okayama University, Okayama 700-8530, Japan
44. Department of Earth and Planetary Sciences, University of California, Davis, CA 95616, USA
45. Department of Science and Engineering, National Museum of Nature and Science, Tsukuba 305-0005, Japan
46. Department of Chemistry, Tokyo University of Science; Tokyo 162-8601, Japan
47. School of Earth Sciences and Engineering, Nanjing University, Nanjing 210023, China
48. Department of Earth Science, Tohoku University, Sendai, 980-8578, Japan
49. Department of Earth and Planetary Sciences, Kyushu University, Fukuoka 819-0395, Japan
50. Earth and Planetary Systems Science Program, Hiroshima University, Higashi-Hiroshima, 739-8526, Japan
51. Kanagawa Institute of Technology, Atsugi 243-0292, Japan
52. UTokyo Organization for Planetary and Space Science, The University of Tokyo, Tokyo 113-0033, Japan

aqueous alteration, as has been observed for the isotopic composition of the highly siderophile element Os (Yokoyama *et al.*, 2011). To further investigate the origin of the materials that accreted to form Ryugu, and chemical processes that affected the asteroidal materials after accretion, we have examined the mass independent (nucleosynthetic) Mo isotopic composition of the returned materials.

Results

Experimental details are provided in the Supplementary Information (Experiments). We analysed a 73.5 mg composite sample of four bulk Ryugu samples (A0106, A0106-A0107, C0107, and C0108). Because of the limited quantity of Mo present in the samples, two samples from each of the two Hayabusa2 sampling locations were combined for a single measurement of the mass independent isotopic composition of Mo. In addition to the Ryugu sample, an equivalent mass of the well characterised CV3 carbonaceous chondrite Allende (Smithsonian Allende powder USNM 2359, Split 20, Position 31; ~50 mg in total) was processed at the same time using the same methods in order to validate the analytical methods. The ε^{i}Mo values of the Ryugu composite sample and Allende investigated in this study are provided in Table 1. The comparison to reference data is provided in the Supplementary Information.

The composite sample is characterised by positive ε^{i}Mo values for ^{92}Mo, ^{94}Mo, ^{95}Mo, and ^{97}Mo, all of which are >2 times larger than those for Allende (Fig. 1). The ε^{i}Mo values in the Ryugu composite decrease in the order of ^{92}Mo > ^{94}Mo > ^{95}Mo > ^{97}Mo, suggesting a deficit of *s*-process Mo isotopes compared to terrestrial values. The Ryugu sample plots on the CC line on the ε^{94}Mo-ε^{95}Mo diagram (Fig. 2a), which is consistent with the observation that Ryugu samples are characterised by CC-type ε^{50}Ti-ε^{54}Cr isotopic systematics (Yokoyama *et al.*, 2023a, b). On a plot of ε^{97}Mo *vs.* ε^{92}Mo, the Ryugu sample plots off the mixing line between a representative terrestrial composition and the theoretical *s*-process composition. This may reflect an underestimate of external uncertainties for these isotopes (details are in Supplementary Information Experiments).

Table 1 Molybdenum isotopic compositions for single analyses of bulk samples of Ryugu and the CV3 carbonaceous chondrite Allende.

	ε^{92}Mo	ε^{94}Mo	ε^{95}Mo	ε^{97}Mo
Ryugu	8.8 ± 0.6	7.2 ± 0.3	4.5 ± 0.3	2.2 ± 0.1
Allende	4.5 ± 0.6	3.0 ± 0.3	2.5 ± 0.3	0.6 ± 0.1

Mo isotope ratios are normalized to ^{98}Mo/^{96}Mo =1.453173. Uncertainties reported for measured ε^{i}Mo values represent the external reproducibility (2 s.d.) obtained from repeated analyses of Highland Valley molybdenite (Table S-4).

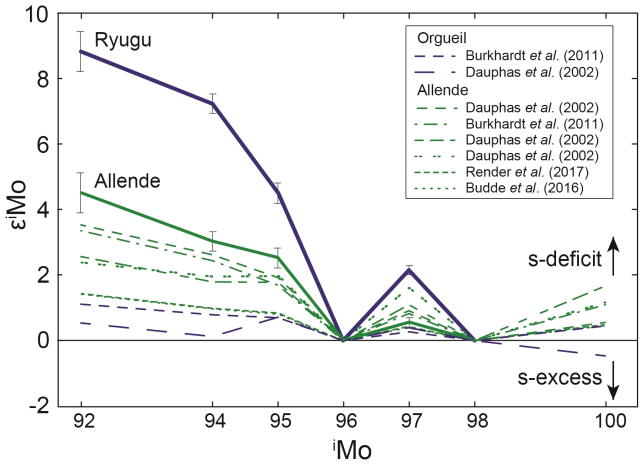

Figure 1 Molybdenum isotopic compositions of Ryugu and Allende analysed in this study (solid lines). The dotted lines represent comparison bulk meteorite data for Allende (green) and Orgueil (blue) from previous studies (Table S-1). Note that ^{100}Mo was not measured in this study.

Discussion

While the Ryugu composite plots on the ε^{94}Mo-ε^{95}Mo CC trend, its ε^{92}Mo, ε^{94}Mo, ε^{95}Mo, and ε^{97}Mo values are all greater than any other "bulk" samples of meteorites previously analysed (Fig. 2b-d), including the CI chondrite Orgueil, which is characterised as having the smallest *s*-process deficit among carbonaceous chondrites (Fig. 2, Dauphas *et al.*, 2002; Burkhardt *et al.*, 2011). The values are also larger than any known iron meteorites (*e.g.*, Kruijer *et al.*, 2017; Bermingham *et al.*, 2018). Determining the cause of the extreme Mo isotope anomaly is an important aspect of fully understanding the origin and internal evolution of Ryugu. As follows, we consider four possible explanations for the large *s*-process deficits in the Ryugu composite sample: 1) biased sampling of chondritic components incorporated in the Ryugu composite sample, 2) the observed isotopic composition represents the original bulk composition of the asteroid Ryugu, 3) incomplete dissolution of presolar SiC grains during the acid digestion steps, and 4) heterogeneous distribution of Mo isotopes in the Ryugu body driven by aqueous alteration processes.

The first potential explanation is that, in the small amount of material analysed, we over-sampled a chondritic component with strong deficits in *s*-process Mo isotopes. This could lead to a bias in the composition of a presumed "bulk" sample of Ryugu. Although Mo isotope data are limited for chondrite components, no known components provide a viable explanation for the Ryugu data. For instance, *s*-process-depleted Mo isotopic compositions have been reported for Allende chondrules (Budde *et al.*, 2016), however, the Allende chondrules have ε^{94}Mo values ranging only from +1.9 to +6.1, all of which are lower than the Ryugu composite (ε^{94}Mo = +7.2 ± 0.3). Most calcium-aluminum inclusions (CAIs) have even smaller positive εMo values (ε^{94}Mo < +2) than chondrules (Burkhardt *et al.*, 2011; Shollenberger *et al.*, 2018; Brennecka *et al.*, 2020). Only a single CAI examined by Burkhardt *et al.* (2011) showed strong deficits of *s*-process Mo isotopes (ε^{94}Mo = +16.8 ± 0.4), however, ~10 % of the analysed Ryugu sample would have to consist of such exotic material to explain the measured Ryugu composition. In addition to the isotopic mismatch, the chemical data for equivalent bulk samples provide no evidence for over-sampling of chondrules or refractory inclusions (Yokoyama *et al.*, 2023a). Further, petrographic observation shows that Ryugu samples, as with all CI chondrites, lack chondrules, CAIs, and metals (*e.g.*, Kawasaki *et al.*, 2022), hence, the components necessary to cause a biased analysis are absent. We conclude that it is unlikely that the observed extreme Mo isotopic anomalies were due to the preferential sampling of precursor chondrite components.

It is also possible that the bulk asteroid Ryugu is characterised by strong *s*-process depletion in certain elements. This could mean that Ryugu formed from proportions of nebular materials that were significantly different from those incorporated in CI meteorites. As noted, Ryugu is characterised by

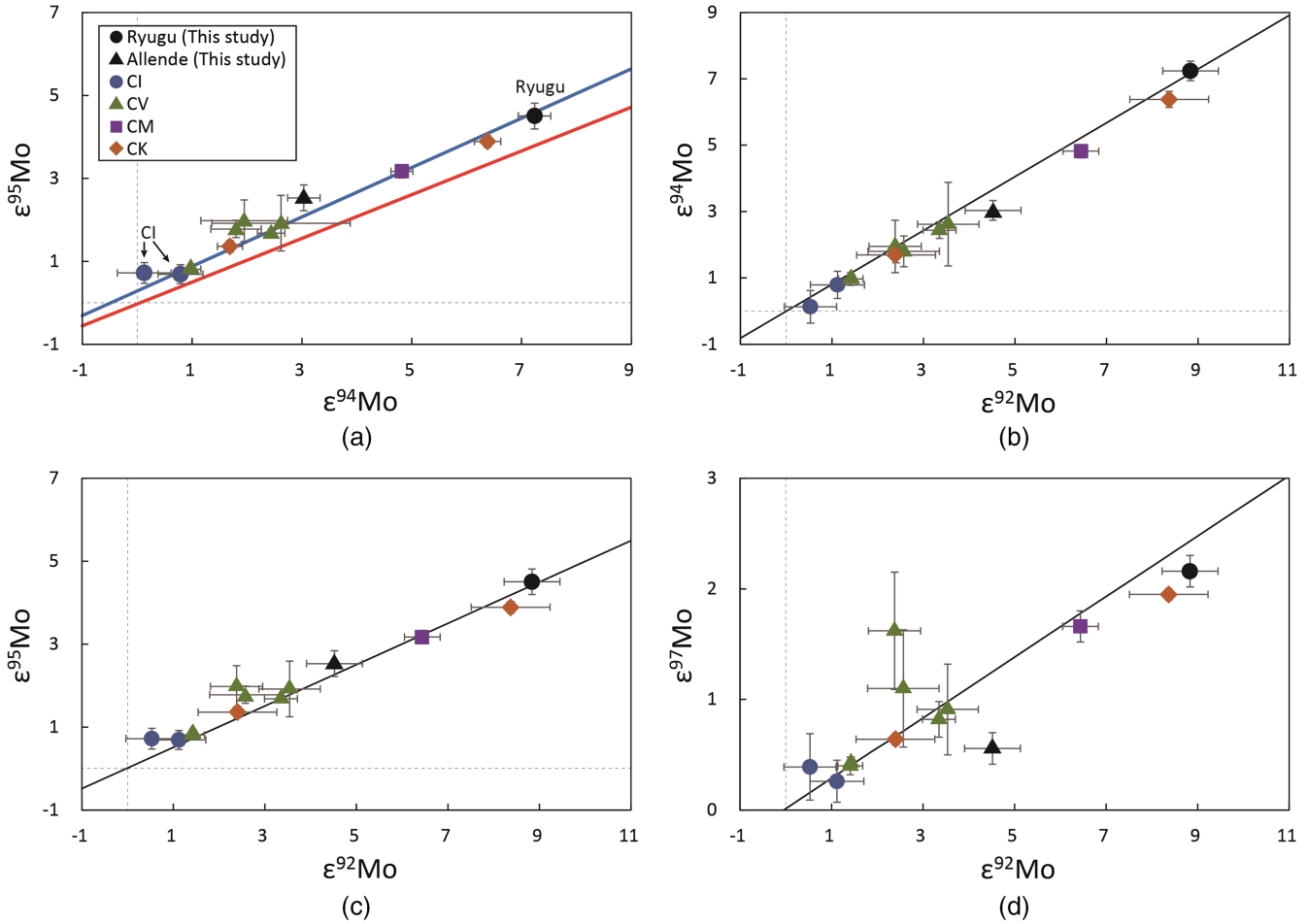

Figure 2 Molybdenum isotope diagrams of bulk meteorites and the Ryugu sample. **(a)** The solid lines are the regression lines of CC (blue, from Budde *et al.*, 2019) and NC (red, from Spitzer *et al.*, 2020) meteorites. **(b), (c), (d)** Reference data of bulk carbonaceous chondrites as listed in Table S-1. Black lines are extensions of the mixing lines between a representative terrestrial sample (origin) and the theoretical *s*-process Mo isotopic composition calculated by Stephan *et al.* (2019).

CI-like nucleosynthetic isotope anomalies in Cr, Ti, Fe, and Zn (*e.g.*, Hopp *et al.*, 2022). The inconsistency between these elements and Mo may suggest that lithophile and siderophile element-rich presolar materials were either differentially distributed within the nebula, or differentially extracted from the nebula during planetesimal accretion. Hopp *et al.*, (2022) found that Ryugu and CI data have identical μ^{54}Fe-μ^{50}Ti values, but the values are distinct from other CC and NC meteorites. These authors suggested that Ryugu and CI parent bodies formed in a nebular region that was different from the source of other carbonaceous asteroids. If however the measured Mo isotopic composition accurately reflects the composition of the bulk Ryugu asteroid, the formation region(s) of Ryugu and CI parent bodies would have to have been heterogeneous with respect to Mo isotopic compositions. Given the strong genetic similarities between Ryugu and CI, we consider it unlikely that bulk Ryugu has a unique Mo isotopic composition.

Certain types of presolar grains may be resistant to the acid digestion methods employed here (Nittler, 2003). Hence, one possible explanation for the extreme *s*-process depletion is incomplete dissolution of presolar SiC grains during the sample digestion steps. This follows from the observation that the majority of presolar SiC grains are characterised by strongly *s*-process-enriched compositions. A sequential acid leaching study of the CI chondrite Orgueil showed that a phase accessed by leaching with 3 M HCl-13.5 M HF was strongly enriched in *s*-process Mo isotopes (ε^{94}Mo = −31.76 ± 0.89), which was most likely contributed by the partial dissolution of presolar SiC (Dauphas *et al.*, 2002). Stephan *et al.* (2019) and Liu *et al.* (2019) reported Mo isotopic anomalies directly measured in single SiC grains, with ε^{94}Mo values ranging from −228 to −9138.

In order to assess the possible effects of incomplete digestion of presolar SiC, we conducted a mass balance calculation assuming that the true bulk Ryugu sample had CI-like Mo isotopic composition. The detailed calculations and assumptions are described in Supplementary Information (mass balance calculation). It should be noted that the Mo isotopic composition of the CI chondrite component used in the calculation is taken from the value for bulk Orgueil (CI) determined by the laser fusion method (Burkhardt *et al.*, 2011). Of note, Dauphas *et al.* (2002) also reported Mo isotopic data for a bulk sample of Orgueil using an acid digestion method. Both laser fusion and acid digestion methods gave generally consistent isotopic compositions (Fig. 1).

Mass balance calculations indicate that, depending on the Mo abundance present in the presolar SiC, anywhere from ~20 to 100 % of the presolar SiC present in the Ryugu sample would have to remain undissolved in order to reduce the *s*-process deficits in Mo to the level of CI chondrites. Given the concordance of the prior analyses of bulk CI meteorites using two different digestion methods, this seems unlikely. Nevertheless, considering the large uncertainties on the assumptions, we cannot rule out this possibility. Although for this study the sample powders

were treated with multiple acid digestion steps, including an HF-HNO_3 heating step at 180 °C, a complete digestion technique applied to Ryugu materials (*e.g.*, alkaline fusion) will ultimately be required to further assess this possibility.

Finally, we consider a scenario in which aqueous alteration and deposition of secondary minerals caused the redistribution of *s*-process-depleted Mo within the Ryugu parent body. Yokoyama *et al.* (2023b) reported that Ryugu materials and CI chondrites show variable ε^{54}Cr values and suggested that fluid driven decoupling *via* parent body aqueous alteration between Cr in chemically labile phases with a slightly negative ε^{54}Cr value, and ^{54}Cr-rich Cr oxide nanoparticles, resulted in mm scale ε^{54}Cr variability in the bulk Ryugu samples and CI chondrites. If this scenario explains the Mo isotopic variation between the Ryugu samples and CI chondrites, the analysed composite sample, consisting of the ~70 mg of Ryugu material, does not represent the bulk Ryugu parent body, but would be dominated by materials depleted in *s*-process-rich presolar grains, likely including SiC, and enriched in the secondary minerals. Sequential acid leaching experiments on CI and CM chondrites revealed that the early stage leaching fractions with mild acids (*e.g.*, CH_3COOH, 4M HNO_3) are characterised by positive εMo values up to *e.g.*, ε^{94}Mo = +24 (Dauphas *et al.*, 2002; Burkhardt *et al.*, 2011). These experimental results demonstrate that easily leachable phases in CI and CM chondrites, possibly aqueously formed secondary carbonates and sulfides, are depleted in *s*-process Mo isotopes. It is, therefore, conceivable that the pervasive aqueous fluid present in the Ryugu parent body, as suggested by Nakamura *et al.* (2023), preferentially dissolved *s*-process depleted, chemically labile phases in the protolith (*e.g.*, amorphous silicates), releasing this Mo into the fluid for transport and deposition elsewhere in the body. One Ryugu sample (C0002) examined by Yokoyama *et al.* (2023b) was characterised by a substantially higher ε^{54}Cr value compared to four other Ryugu samples (A0106, A0106-A0107, C0107, and C0108), presumably due to the low abundance of the secondary minerals (*e.g.*, dolomite) in the sample. This suggests that the isotopic composition of Cr may be correlated with the abundance of secondary minerals. Although C0002 was not analysed for Mo in this study, it might be predicted that this sample was also enriched in *s*-process Mo isotopes compared to the Ryugu materials examined in this study. It should be noted that Barosch *et al.* (2022) reported the average SiC abundance of 25 ppm in Ryugu samples is consistent with the average value of 23 ppm in CI chondrites, however, given the limited area analysed, future additional analyses will be required to assess the heterogeneity of presolar materials in the Ryugu samples. A detailed mechanism that would result in the separation of complementary *s*-process depleted Mo from domains with *s*-process-rich presolar grains and the secondary minerals remains unclear.

We conclude that the most likely cause for the extreme mass independent Mo isotopic composition of a composite sample of Ryugu is fluid redistribution of *s*-process depleted Mo in the asteroid. Alternatively, incomplete digestion of presolar SiC is also possible. None of the four options, however, can be fully dismissed at this time. Additional analyses using more rigorous digestion methods and/or acid leaching methods might reveal whether resistance of SiC grains to dissolution led to the strong *s*-process depletion. Analyses of different Ryugu samples would also provide important constraints on whether the Ryugu body was formed from CI-like materials, but with heterogeneous Mo isotopic composition at the ~70 mg level, or the Ryugu body was formed from highly *s*-process depleted materials. In the case of the former, isotopic variations might be correlated with variations in bulk chemical compositions of individual samples (*e.g.*, proxies for aqueous alteration or redistribution). In the case of the latter, isotopic homogeneity would be expected for multiple samples. If homogeneity of multiple samples was demonstrated, it might therefore, suggest a different origin for the siderophile Mo in Ryugu relative to the lithophile elements that have been measured for nucleosynthetic isotopic compositions (Cr, Ti, Fe, and Zn). Analysis of the isotopic compositions of Ru and W would then be useful given their similar, siderophile element chemical characteristics to Mo.

Acknowledgments

Hayabusa2 was developed and built under the leadership of Japan Aerospace Exploration Agency (JAXA), with contributions from the German Aerospace Center (DLR) and the Centre National d'Études Spatiales (CNES), and in collaboration with NASA, and other universities, institutes, and companies in Japan. The curation system was developed by JAXA in collaboration with companies in Japan. The Smithsonian National Museum of Natural History is also acknowledged for providing the Allende powder. We thank three anonymous reviewers for their helpful comments. We also thank H.A. Tornabene, and K.R. Bermingham for the chemical processing of Highland Valley molybdenite, and R.D. Ash, and J.L. Hellmann for help with the MC-ICP-MS measurements. This research was supported by NASA Emerging Worlds grant (80NSSC20K0335 to RJW) and JSPS KAKENHI grants (18H01258, 19H00715, 20H04609, and 21KK0058 to TY).

Editor: Francis McCubbin

Additional Information

Supplementary Information accompanies this letter at https://www.geochemicalperspectivesletters.org/article2341.

Cite this letter as: Nakanishi, N., Yokoyama, T., Ishikawa, A., Walker, R.J., Abe, Y., *et al.* (2023) Nucleosynthetic *s*-Process Depletion in Mo from Ryugu samples returned by Hayabusa2. *Geochem. Persp. Let.* 28, 31–36. https://doi.org/10.7185/geochemlet.2341

References

Barosch, J., Nittler, L.R., Wang, J., Alexander, C.M.O.'D., De Gregorio, B.T., *et al.* (2022) Presolar Stardust in Asteroid Ryugu. *The Astrophysical Journal Letters* 935, L3. https://doi.org/10.3847/2041-8213/ac83bd

Bermingham, K.R., Worsham, E.A., Walker, R.J. (2018) New insights into Mo and Ru isotope variation in the nebula and terrestrial planet accretionary genetics. *Earth and Planetary Science Letters* 487, 221–229. https://doi.org/10.1016/j.epsl.2018.01.017

Brennecka, G.A., Burkhardt, C., Budde, G., Kruijer, T.S., Nimmo, F., Kleine, T. (2020) Astronomical context of Solar System formation from molybdenum isotopes in meteorite inclusions. *Science* 370, 837–840. https://doi.org/10.1126/science.aaz8482

Budde, G., Burkhardt, C., Brennecka, G.A., Fischer-Gödde, M., Kruijer, T.S., Kleine, T. (2016) Molybdenum isotopic evidence for the origin of

chondrules and a distinct genetic heritage of carbonaceous and non-carbonaceous meteorites. *Earth and Planetary Science Letters* 454, 293–303. https://doi.org/10.1016/j.epsl.2016.09.020

Budde, G., Burkhardt, C., Kleine, T. (2019) Molybdenum isotopic evidence for the late accretion of outer Solar System material to Earth. *Nature Astronomy* 3, 736–741. https://doi.org/10.1038/s41550-019-0779-y

Burkhardt, C., Kleine, T., Oberli, F., Pack, A., Bourdon, B., Wieler, R. (2011) Molybdenum isotope anomalies in meteorites: Constraints on solar nebula evolution and origin of the Earth. *Earth and Planetary Science Letters* 312, 390–400. https://doi.org/10.1016/j.epsl.2011.10.010

Bus, S.J., Binzel, R.P. (2002) Phase II of the small main-belt asteroid spectroscopic survey. A feature-based taxonomy. *Icarus* 158, 146–177. https://doi.org/10.1006/icar.2002.6856

Dauphas, N., Schauble, E.A. (2016) Mass Fractionation Laws, Mass-Independent Effects, and Isotopic Anomalies. *Annual Review of Earth and Planetary Sciences* 44, 709–783. https://doi.org/10.1146/annurev-earth-060115-012157

Dauphas, N., Marty, B., Reisberg, L. (2002) Molybdenum Nucleosynthetic Dichotomy Revealed in Primitive Meteorites. *The Astrophysical Journal* 569, L139–L142. https://doi.org/10.1086/340580

Hopp, T., Dauphas, N., Abe, Y., Aléon, J., Alexander, C.M.O.'D., *et al.* (2022) Ryugu's nucleosynthetic heritage from the outskirts of the Solar System. *Science Advances* 8, 1–10. https://doi.org/10.1126/sciadv.add8141

Kadlag, Y., Becker, H., Harbott, A. (2019) Cr isotopes in physically separated components of the Allende CV3 and Murchison CM2 chondrites: Implications for isotopic heterogeneity in the solar nebula and parent body processes. *Meteoritics & Planetary Science* 54, 2116–2131. https://doi.org/10.1111/maps.13375

Kawasaki, N., Nagashima, K., Sakamoto, N., Matsumoto, T., Bajo, K.I., *et al.* (2022) Oxygen isotopes of anhydrous primary minerals show kinship between asteroid Ryugu and comet 81P/Wild2. *Science Advances* 8, eade2067. https://doi.org/10.1126/sciadv.ade2067

Kruijer, T.S., Burkhardt, C., Budde, G., Kleine, T. (2017) Age of Jupiter inferred from the distinct genetics and formation times of meteorites. *Proceedings of the National Academy of Sciences* 114, 201704461. https://doi.org/10.1073/pnas.1704461114

Liu, N., Stephan, T., Cristallo, S., Gallino, R., Boehnke, P., *et al.* (2019) Presolar Silicon Carbide Grains of Types Y and Z: Their Molybdenum Isotopic Compositions and Stellar Origins. *The Astrophysical Journal* 881, 28. https://doi.org/10.3847/1538-4357/ab2d27

Moynier, F., Dai, W., Yokoyama, T., Hu, Y., Paquet, M., *et al.* (2022) The Solar System calcium isotopic composition inferred from Ryugu samples. *Geochemical Perspectives Letters* 24, 1–6. https://doi.org/10.7185/geochemlet.2238

Nakamura, E., Kobayashi, K., Tanaka, R., Kunihiro, T., Kitagawa, H., *et al.* (2022) On the origin and evolution of the asteroid Ryugu: A comprehensive geochemical perspective. *Proceedings of the Japan Academy. Series B, Physical and Biological Sciences* 98, 227–282. https://doi.org/10.2183/pjab.98.015

Nakamura, T., Matsumoto, M., Amano, K., Enokido, Y., Zolensky, M.E., *et al.* (2023) Formation and evolution of carbonaceous asteroid Ryugu: Direct evidence from returned samples. *Science* 379, eabn8671. https://doi.org/10.1126/science.abn8671

Nittler, L.R. (2003) Presolar stardust in meteorites: recent advances and scientific frontiers. *Earth and Planetary Science Letters* 209, 259–273. https://doi.org/10.1016/S0012-821X(02)01153-6

Paquet, M., Moynier, F., Yokoyama, T., Dai, W., Hu, Y., *et al.* (2023) Contribution of Ryugu-like material to Earth's volatile inventory by Cu and Zn isotopic analysis. *Nature Astronomy* 7, 182–189. https://doi.org/10.1038/s41550-022-01846-1

Poole, G.M., Rehkämper, M., Coles, B.J., Goldberg, T., Smith, C.L. (2017) Nucleosynthetic molybdenum isotope anomalies in iron meteorites – new evidence for thermal processing of solar nebula material. *Earth and Planetary Science Letters* 473, 215–226. https://doi.org/10.1016/j.epsl.2017.05.001

Render, J., Fischer-Gödde, M., Burkhardt, C., Kleine, T. (2017) The cosmic molybdenum-neodymium isotope correlation and the building material of the Earth. *Geochemical Perspectives Letters* 3, 170–178. https://doi.org/10.7185/geochemlet.1720

Shollenberger, Q.R., Borg, L.E., Render, J., Ebert, S., Bischoff, A., Russell, S.S., Brennecka, G.A. (2018) Isotopic coherence of refractory inclusions from CV and CK meteorites: Evidence from multiple isotope systems. *Geochimica et Cosmochimica Acta* 228, 62–80. https://doi.org/10.1016/j.gca.2018.02.006

Spitzer, F., Burkhardt, C., Budde, G., Kruijer, T. S., Morbidelli, A., Kleine, T. (2020) Isotopic Evolution of the Inner Solar System Inferred from Molybdenum Isotopes in Meteorites. *The Astrophysical Journal* 898, L2. https://doi.org/10.3847/2041-8213/ab9e6a

Stephan, T., Trappitsch, R., Hoppe, P., Davis, A.M., Pellin, M.J., Pardo, O.S. (2019) Molybdenum Isotopes in Presolar Silicon Carbide Grains: Details of s-process Nucleosynthesis in Parent Stars and Implications for r- and p-processes. *The Astrophysical Journal* 877, 101. https://doi.org/10.3847/1538-4357/ab1c60

Tachibana, S., Sawada, H., Okazaki, R., Takano, Y., Sakamoto, K., *et al.* (2022) Pebbles and sand on asteroid (162173) Ryugu: In situ observation and particles returned to Earth. *Science* 375, 1011–1016. https://doi.org/10.1126/science.abj8624

Williams, C.D., Sanborn, M.E., Defouilloy, C., Yin, Q.Z., Kita, N.T., Ebel, D.S., Yamakawa, A., Yamashita, K. (2020) Chondrules reveal large-scale outward transport of inner Solar System materials in the protoplanetary disk. *Proceedings of the National Academy of Sciences of the United States of America* 117, 23426–23435. https://doi.org/10.1073/pnas.2005235117

Worsham, E.A., Bermingham, K.R., Walker, R.J. (2017) Characterizing cosmochemical materials with genetic affinities to the Earth: Genetic and chronological diversity within the IAB iron meteorite complex. *Earth and Planetary Science Letters* 467, 157–166. https://doi.org/10.1016/j.epsl.2017.02.044

Yokoyama, T., Walker, R.J. (2016) Nucleosynthetic Isotope Variations of Siderophile and Chalcophile Elements in the Solar System. *Reviews in Mineralogy & Geochemistry* 81, 107–160. https://doi.org/10.2138/rmg.2016.81.03

Yokoyama, T., Alexander, C.M.O.'D., Walker, R.J. (2011) Assessment of nebular versus parent body processes on presolar components present in chondrites: Evidence from osmium isotopes. *Earth and Planetary Science Letters* 305, 115–123. https://doi.org/10.1016/j.epsl.2011.02.046

Yokoyama, T., Nagai, Y., Fukai, R., Hirata, T. (2019) Origin and Evolution of Distinct Molybdenum Isotopic Variabilities within Carbonaceous and Noncarbonaceous Reservoirs. *The Astrophysical Journal* 883, 62. https://doi.org/10.3847/1538-4357/ab39e7

Yokoyama, T., Nagashima, K., Nakai, I., Young, E.D., Abe, Y., *et al.* (2023a) Samples returned from the asteroid Ryugu are similar to Ivuna-type carbonaceous meteorites. *Science* 379, eabn7850. https://doi.org/10.1126/science.abn7850

Yokoyama T., Wadhwa, M., Iizuka, T., Abe Y., Aléon J., *et al.* (2023b) Water circulation in Ryugu asteroid affected the distribution of nucleosynthetic isotope anomalies in returned sample. *Science Advances* 9, eadi7048. https://doi.org/10.1126/sciadv.adi7048

Geochemical Perspectives Letters

Nucleosynthetic s-Process Depletion in Mo from Ryugu samples returned by Hayabusa2

N. Nakanishi, T. Yokoyama, A. Ishikawa, R.J. Walker, Y. Abe, J. Aléon, C.M.O'D Alexander, S. Amari, Y. Amelin, K.-I. Bajo, M. Bizzarro, A. Bouvier, R.W. Carlson, M. Chaussidon, B.-G. Choi, N. Dauphas, A.M. Davis, T. Di Rocco, W. Fujiya, R. Fukai, I. Gautam, M.K. Haba, Y. Hibiya, H. Hidaka, H. Homma, P. Hoppe, G.R. Huss, K. Ichida, T. Iizuka, T.R. Ireland, S. Itoh, N. Kawasaki, N.T. Kita, K. Kitajima, T. Kleine, S. Komatani, A.N. Krot, M.-C. Liu, Y. Masuda, M. Morita, K. Motomura, F. Moynier, I. Nakai, K. Nagashima, A. Nguyen, L. Nittler, M. Onose, A. Pack, C. Park, L. Piani, L. Qin, S.S. Russell, N. Sakamoto, M. Schönbächler, L. Tafla, H. Tang, K. Terada, Y. Terada, T. Usui, S. Wada, M. Wadhwa, K. Yamashita, Q.-Z. Yin, S. Yoneda, E.D. Young, H. Yui, A.-C. Zhang, T. Nakamura, H. Naraoka, T. Noguchi, R. Okazaki, K. Sakamoto, H. Yabuta, M. Abe, A. Miyazaki, A. Nakato, M. Nishimura, T. Okada, T. Yada, K. Yogata, S. Nakazawa, T. Saiki, S. Tanaka, F. Terui, Y. Tsuda, S.-I. Watanabe, M. Yoshikawa, S. Tachibana, H. Yurimoto

Supplementary Information

The Supplementary Information includes:

- Experiments
- Results of Allende
- Mass balance calculation
- Tables S-1 to S-4
- Supplementary Information References

Experiments

Four bulk Ryugu samples (A0106 and A0106-A0107 from Chamber A, C0107 and C0108 from Chamber C) and two Allende samples (Allende A and Allende B) were examined in this study. The Ryugu sample A0106-A0107 was a powdered material prepared from a mixed aggregate of A0106 (1.6 mg) and A0107 (27 mg), such that 94% of this material was composed of A0107. The sample C0108 was a powdered material retrieved from a sealed cell used in the XRF analysis (Yokoyama *et al*., 2023).

The Ryugu samples A0106 and C0107 were residues obtained after extracting soluble organic matter (SOM) using hexane, dichloromethane, and methanol (Yoshimura *et al*., 2023). To estimate the removal rate of Mo in individual extraction processes with the organic solvents, we conducted a SOM extraction test using 43.73 mg of powdered Tagish Lake (C2 ungrouped). Tagish Lake has similar lithologies and mineralogies to CI chondrites and Ryugu, although Tagish Lake has sparse chondrule-like objects and altered CAIs. The Mo yields in individual organic solvents are listed in Table S-2. The total amount of Mo removed by the three-step SOM extraction procedures were less than 0.2%. An earlier leaching experiment on CI chondrite Orgueil (Dauphas *et al*., 2002) showed that the Mo isotopic compositions of the first leachate (8.5 M CH_3COOH, 20 °C, 1 day) were generally within uncertainties of the terrestrial value. Therefore, we conclude that the Mo isotopic compositions of Ryugu samples A0106 and C0107 were not significantly modified by the SOM extraction steps.

The weight of each Ryugu sample dedicated for acid digestion was 23.88, 22.24, 14.61, and 12.78 mg for A0106-A0107, C0108, A0106, and C0107, respectively. Additionally, we examined two aliquots of the Smithsonian Allende powder (USNM 2359, Split 20, Position 31; 19.94 and 32.46 mg, 52.4 mg in total).

Sample digestion and the first and second steps of the chemical separation were conducted at the Tokyo Institute of Technology (Tokyo Tech), of which the details are described in Yokoyama *et al*. (2023). The powdered samples were weighed in Teflon vials and heated with a mixture of 0.25 mL HF and 0.25 mL HNO_3 at 180 °C for 5 days and dried. After digestion, a mixture of 0.1 mL HNO_3 and 0.1 mL HCl was added to each sample, heated at 110 °C for two days, and dried. Then, a mixture of 0.35 mL HNO_3, 0.1 mL H_2O_2, and 0.2 mL H_2O was added to each sample, heated at 90 °C for two days, and dried. The dissolved sample was conditioned with 1 mL 1.5 M HBr, which was loaded onto 0.1 mL of an anion exchange resin (AG1-X8, 200–400 mesh, BioRad). Major element cuts containing Mo were collected with 0.45 mL 1.5 M HBr. The major element cut was dried and conditioned with 1 mL 0.4 M HCl–0.5 M HF, which was loaded onto 1 mL of anion exchange resin. Molybdenum was separated from most of the other elements by this step (Nagai and Yokoyama, 2014). The Mo recovery yields during chemistries performed at Tokyo Tech were ~85%.

After the initial Mo separation at Tokyo Tech, the samples were transferred to the University of Maryland (UMd). Because the separated samples contained insufficient Mo for measuring isotope ratios individually to a meaningful precision, the four Ryugu samples and the two Allende samples were respectively combined at UMd. The composite samples were dissolved in 0.5M HCl-0.5 M HF, and Mo was further purified using anion exchange column chemistry as described in (Nagai and Yokoyama, 2014). The column separations were repeated to reduce Zr and Ru abundances. Approximately 50 ng and 55 ng of Mo were purified from ~70 mg of the Ryugu powdered samples and ~50 mg of the Allende sample powder, respectively. The Mo recovery yields during chemistries performed at UMd were ~90%.

The total procedural blanks for the chemistries performed at Tokyo Tech are listed in Table S-3. A0106-A0107 and C0108, and A0106 and C0107 were processed in round 1 and 2, respectively. Although

the blanks for round 2 do not include the SOM extraction steps, Mo blanks in 2 mL of each organic reagent were measured (Table S-3). All three organic reagents used in SOM extraction contain little Mo. Because the four Ryugu samples were combined at UMd, the total Mo blank during the process at Tokyo Tech is estimated to be 5.7 ng. The additional blank added at UMd as a result of further processing is estimated to be 0.4 ng. Assuming the blanks have terrestrial isotopic composition, blank corrections change the ε^{i}Mo values of the Ryugu composite sample and Allende further above the CC line.

Molybdenum isotopic compositions were measured using a *Neptune Plus* multi-collector inductively-coupled plasma mass spectrometer (MC-ICP-MS, *Thermo Fisher*) at UMd. Ion beams of ^{92}Mo, ^{94}Mo, ^{95}Mo, ^{97}Mo, and ^{98}Mo were analyzed on Faraday collectors coupled with 10^{11} Ω amplifiers. Isobaric interferences from Zr and Ru were collected by monitoring ^{91}Zr and ^{99}Ru using 10^{13} Ω amplifiers. Due to the limited number of 10^{11} Ω amplifiers, ^{100}Mo was not measured. Because the samples consisted of limited Mo, an X-skimmer cone and H-sample cone combination was used for greatest sensitivity. The purified Mo solutions (50 ppb in 0.5 M HNO_3-0.05 M HF) were introduced into the MC-ICP-MS using an *Aridus 2* (*CETAC Technologies*) desolvating nebulizer. The 50 ppb solutions gave signals of 2 V on ^{98}Mo for over 100 cycles with 8.4 s integration times. Sample analyses were bracketed by measurements of an *Alfa Aesar* Mo standard solution. A terrestrial sample of 200 Ma molybdenite (Highland Valley) was measured in the same session as the Ryugu sample to assess the accuracy and precision of the measurements. The Highland Valley molybdenite was digested with HNO_3 and HCl and processed through a primary column before the measurements. The sample was previously measured numerous times in the UMd laboratory using thermal ionization mass spectrometry in negative ionization mode (N-TIMS) using a *Thermo Fisher Triton Plus* (Bermingham *et al*., 2018).

The results for the molybdenite are summarized in Table S-4. The Mo isotopic ratios are reported as ε^{i}Mo values ($\varepsilon^{i}Mo = [(^{i}Mo/^{96}Mo)_{sample}/(^{i}Mo/^{96}Mo)_{standard} - 1] \times 10^{4}$) for ^{92}Mo, ^{94}Mo, ^{95}Mo, and ^{97}Mo. The results for the molybdenite were in good agreement with the previous measurements. The analytical reproducibilities (2SD) as estimated by repeated analyses of equivalent quantities of Highland Valley (n = 6)

to the Ryugu and Allende samples are ± 0.6 for ε^{92}Mo, ± 0.3 for ε^{94}Mo, ± 0.3 for ε^{95}Mo, and ± 0.1 for ε^{97}Mo. It should be noted that these 2SDs are minimum estimates for the true external reproducibility. Because the Ryugu and Allende samples have complex matrices, the samples required more complex digestion and separation steps than the molybdenite. Due to the coexistence of Zr and Ru in the measured Mo samples for Allende (Zr/Mo = 0.0011, Ru/Mo = 0.0004) and Ryugu (Zr/Mo = 0.0010, Ru/Mo = 0.0002), relatively, large interference corrections were made on the obtained ε^{92}Mo, ε^{94}Mo, ε^{95}Mo, and ε^{97}Mo values, which were -11 ε, -20 ε, 3 ε, and 3 ε for Allende and -10 ε, -18 ε, 3 ε, and 3 ε for Ryugu.

Results of Allende

The Mo isotopic pattern of Allende is characterized by positive ε^{i}Mo values that decrease in the order of ^{92}Mo > ^{94}Mo > ^{95}Mo > ^{97}Mo with a kink at ^{94}Mo and ^{95}Mo (Fig. 1), suggesting a combination of both *s*-process deficit and *r*-process excess in Mo isotopes compared to the terrestrial standard. The ε^{92}Mo, ε^{94}Mo, and ε^{95}Mo values of Allende were slightly higher than the range of literature values (Dauphas *et al*., 2002; Burkhardt *et al*., 2011; Budde *et al*., 2016; Render *et al*., 2017), while the obtained ε^{97}Mo value was slightly lower than the literature values. The difference is not due to an inadequate interference correction of Zr^{+} and Ru^{+} ions, because the correction lowers the observed ε^{92}Mo and ε^{94}Mo values but increases the ε^{95}Mo value. Given the small sample size of the Allende sample examined in this study (52.4 mg), this difference most likely reflects compositional heterogeneities in Allende consistent with powders including greater or lesser proportions of chondrules, calcium aluminum inclusions (CAIs) and amoeboid olivine aggregates (AOAs). For example, chondrule fractions separated from Allende show *s*-deficit compositions ranging from + 1.42 to + 3.98 on ε^{95}Mo (Budde *et al*., 2016). Therefore, the Allende samples measured in previous studies may have originally contained slightly lower proportions of chondrule-like materials than the Allende reference powder measured in this study. Previous studies have shown that Mo isotopic data for CC and NC meteorites define two distinct linear trends on the ε^{94}Mo-ε^{95}Mo diagram (Budde *et al*., 2016; Poole *et al*., 2017; Worsham *et al*., 2017). The

Allende sample generally plots on the CC line (Fig. 2a) as is consistent with prior studies and validates our Mo isotope analysis methods using multi-collector inductively-coupled plasma mass spectrometry (MC-ICP-MS). The observation that the datum plots slightly above the line, most likely due to an excess of *r*-process Mo, may indicate that the Allende sample aliquot analyzed was enriched in CAI material compared to the Allende samples measured in previous studies.

Mass balance calculation

For the calculations we assumed: 1) δ^{92}Mo, δ^{94}Mo, δ^{95}Mo, δ^{97}Mo, and δ^{98}Mo values for SiC to average -686, -662, -418, -356, and -167, respectively (*e.g.*, Stephan *et al*., 2019; Liu *et al*., 2019), 2) a SiC abundance of 25 ppm in bulk Ryugu, as determined from the total area of ~39,000 μm^2 in Ryugu thin section and pressed particles (Barosch *et al*., 2022), 3) the measured Mo abundance of 1 μg/g for the Ryugu sample (Yokoyama *et al*., 2023), and 4) the range of Mo abundances previously reported for presolar SiC (10-100 μg/g; Nicolussi *et al*., 1998). We note that the Mo concentration in presolar SiC is not well determined.

For MC-ICP-MS and TIMS measurements, all the ε^{i}Mo values were determined by applying the mass fractionation correction. On the other hand, in resonance ionization mass spectrometry, which is used for analyses of SiC grains, the mass fractionation can be corrected using external standards, and the remaining natural mass fractionation is negligible relative to large nucleosynthesis anomalies of SiC grains. Thus, the MC-ICP-MS and TIMS data need to be transformed to values without internal normalization so that they can be compared with SiC grain data (Lugaro *et al*., 2023; Stephan and Davis, 2021). Using these values, the compositions of the mixture of Ryugu material and presolar SiC at each SiC mixing rate. The SiC mixing rate (Ryugu 1 mol *vs.* SiC X mol) was increased by 0.00002 for each step of the calculation.

Supplementary Tables

Table S-1 Bulk meteorite data from previous studies.

	ε^{92}Mo	ε^{94}Mo	ε^{95}Mo	ε^{97}Mo	ε^{100}Mo
Allende (CV)					
Dauphas *et al*. (2002)	2.38 ± 0.57	1.95 ± 0.79	1.98 ± 0.50	1.62 ± 0.53	1.17 ± 0.50
Dauphas *et al*. (2002)	3.54 ± 0.67	2.62 ± 1.26	1.92 ± 0.67	0.91 ± 0.41	0.56 ± 0.52
Dauphas *et al*. (2002)	2.57 ± 0.78	1.80 ± 0.46	1.78 ± 0.21	1.10 ± 0.53	1.67 ± 0.34
Burkhadt *et al.* (2011)	3.35 ± 0.36	2.44 ± 0.25	1.68 ± 0.09	0.82 ± 0.16	1.10 ± 0.14
Budde *et al*. (2016)	1.41 ± 0.27	0.97 ± 0.19	0.81 ± 0.05	0.40 ± 0.08	0.44 ± 0.12
Render *et al*. (2017)	1.43 ± 0.08	0.98 ± 0.05	0.84 ± 0.05	0.43 ± 0.05	0.49 ± 0.10
Orgueil (CI)					
Dauphas *et al*. (2002)	0.53 ± 0.57	0.13 ± 0.49	0.72 ± 0.25	0.39 ± 0.30	-0.47 ± 0.35
Burkhardt *et al*. (2011)	1.12 ± 0.59	0.79 ± 0.41	0.69 ± 0.23	0.26 ± 0.19	0.44 ± 0.34
Murchison (CM)					
Burkhardt *et al*. (2011)	6.44 ± 0.39	4.82 ± 0.2	3.17 ± 0.16	1.66 ± 0.14	2.28 ± 0.22
NWA 6604, DaG 412 (CK)					
Yokoyama *et al*. (2019)	2.4 ± 0.86	1.69 ± 0.23	1.36 ± 0.14	0.64 ± 0.05	0.76 ± 0.24
Yokoyama *et al*. (2019)	8.37 ± 0.86	6.38 ± 0.24	3.89 ± 0.14	1.95 ± 0.05	2.73 ± 0.24

The uncertainties shown are calculated at the 95 % confidence interval or the 2SD.

Table S-2 Recovery yield of Molybdenum (%) during the SOM extraction experiment using 43.73 mg of powdered Tagish Lake.

	Mo (%)
Hexane	0.06
DCM	0.10
MeOH	0.04

Table S-3 Organic reagents and procedural blank results.

		Mo (ng)
Blank in organic reagents		
Hexane		0
Dichloromethane		0
Methanol		0.01
Procedural blank		
Chemistries at Tokyo Tech		
Round-1	TAB-1	2.5
	TAB-2	2.3
Round-2	TAB-3	0.5
	TAB-4	0.4
Chemistries at UMd		
		0.4*

*Estimated from blank values of similar experiments.

Table S-4 Molybdenum isotopic composition for the Highland Valley terrestrial molybdenum sample.

	ε^{92}Mo	ε^{94}Mo	ε^{95}Mo	ε^{97}Mo
	0.35 ± 0.29	0.29 ± 0.20	0.15 ± 0.14	0.00 ± 0.11
	0.28 ± 0.29	0.16 ± 0.18	0.14 ± 0.14	-0.08 ± 0.12
	-0.30 ± 0.33	0.00 ± 0.23	-0.16 ± 0.17	-0.17 ± 0.13
	0.50 ± 0.27	0.12 ± 0.18	0.09 ± 0.13	-0.06 ± 0.10
	0.36 ± 0.29	0.04 ± 0.18	0.03 ± 0.15	-0.04 ± 0.11
	-0.06 ± 0.22	-0.15 ± 0.19	-0.20 ± 0.12	-0.18 ± 0.11
n	6	6	6	6
AVG	0.19	0.08	0.01	-0.09
2SD	0.61	0.30	0.31	0.14
95% conf.	0.32	0.16	0.16	0.07
TIMS data* (n = 2)	0.41 ± 0.76	0.17 ± 0.27	0.03 ± 0.15	-0.05 ± 0.06

Mo isotope ratios are normalized to ^{98}Mo/^{96}Mo =1.453173.
Uncertainties are reported as the 2SE run statistics of individual analyses.
*From Bermingham *et al*. (2018). Errors are 2SD of repeat analyses of the Mo standard solution.

Supplementary Information References

Barosch, J., Nittler, L.R., Wang, J., Alexander, C.M.O.'D., De Gregorio, B.T., *et al.* (2022) Presolar Stardust in Asteroid Ryugu. *The Astrophysical Journal Letters* 935, L3. https://doi.org/10.3847/2041-8213/ac83bd

Bermingham, K.R., Worsham, E.A., Walker, R.J. (2018) New insights into Mo and Ru isotope variation in the nebula and terrestrial planet accretionary genetics. *Earth and Planetary Science Letters* 487, 221–229. https://doi.org/10.1016/j.epsl.2018.01.017

Budde, G., Burkhardt, C., Brennecka, G.A., Fischer-gödde, M., Kruijer, T.S., Kleine, T. (2016) Molybdenum isotopic evidence for the origin of chondrules and a distinct genetic heritage of carbonaceous and non-carbonaceous meteorites. *Earth and Planetary Science Letters* 454, 293–303. https://doi.org/10.1016/j.epsl.2016.09.020

Burkhardt, C., Kleine, T., Oberli, F., Pack, A., Bourdon, B., Wieler, R. (2011) Molybdenum isotope anomalies in meteorites: Constraints on solar nebula evolution and origin of the Earth. *Earth and Planetary Science Letters* 312, 390–400. https://doi.org/10.1016/j.epsl.2011.10.010

Dauphas, N., Marty, B., Reisberg, L. (2002) Molybdenum Nucleosynthetic Dichotomy Revealed in Primitive Meteorites. *The Astrophysical Journal 569*, L139–L142. https://doi.org/10.1086/340580

Liu, N., Stephan, T., Cristallo, S., Gallino, R., Boehnke, P., *et al.* (2019) Presolar Silicon Carbide Grains of Types Y and Z: Their Molybdenum Isotopic Compositions and Stellar Origins. *The Astrophysical Journal* 881, 28. https://doi.org/10.3847/1538-4357/ab2d27

Lugaro, M., Ek, M., Pető, M., Pignatari, M., Makhatadze, G.V., Onyett, I.J., Schönbächler, M. (2023) Representation of s-process abundances for comparison to data from bulk meteorites. *European Physical Journal A*, 59. https://doi.org/10.1140/epja/s10050-023-00968-y

Nagai, Y., Yokoyama, T. (2014) Chemical separation of Mo and W from terrestrial and extraterrestrial samples via anion exchange chromatography. *Analytical Chemistry* 86, 4856–4863. https://doi.org/10.1021/ac404223t

Nicolussi, G.K., Pellin, M.J., Lewis, R.S., Davis, A.M., Amari, S., Clayton, R.N. (1998) Molybdenum isotopic composition of individual presolar silicon carbide grains from the Murchison meteorite. *Geochimica et Cosmochimica Acta* 62, 1093–1104. https://doi.org/10.1016/S0016-7037(98)00038-6

Poole, G.M., Rehkämper, M., Coles, B.J., Goldberg, T., Smith, C.L. (2017) Nucleosynthetic molybdenum isotope anomalies in iron meteorites – new evidence for thermal processing of solar nebula material. *Earth and Planetary Science Letters* 473. https://doi.org/10.1016/j.epsl.2017.05.001

Render, J., Fischer-Gödde, M., Burkhardt, C., Kleine, T. (2017) The cosmic molybdenum-neodymium isotope correlation and the building material of the Earth. *Geochemical Perspectives Letters* 3, 170–178. https://doi.org/10.7185/geochemlet.1720

Stephan, T., Trappitsch, R., Hoppe, P., Davis, A.M., Pellin, M.J., Pardo, O.S. (2019) Molybdenum Isotopes in Presolar Silicon Carbide Grains: Details of s -process Nucleosynthesis in Parent Stars and Implications for r - and p -processes. *The Astrophysical Journal* 877, 101. https://doi.org/10.3847/1538-4357/ab1c60

Stephan, T., Davis, A.M. (2021) Molybdenum Isotope Dichotomy in Meteorites Caused by s-Process Variability. *The Astrophysical Journal* 909, 8. https://doi.org/10.3847/1538-4357/abd725

Worsham, E.A., Bermingham, K.R., Walker, R.J. (2017) Characterizing cosmochemical materials with genetic affinities to the Earth: Genetic and chronological diversity within the IAB iron meteorite complex. *Earth and Planetary Science Letters* 467, 157–166. https://doi.org/10.1016/j.epsl.2017.02.044

Yokoyama, T., Nagai, Y., Fukai, R., Hirata, T. (2019) Origin and Evolution of Distinct Molybdenum Isotopic Variabilities within Carbonaceous and Noncarbonaceous Reservoirs. *The Astrophysical Journal* 883, 62. https://doi.org/10.3847/1538-4357/ab39e7

Yokoyama, T., Nagashima, K., Nakai, I., Young, E.D., Abe, Y., *et al.* (2023) Samples returned from the asteroid Ryugu are similar to Ivuna-type carbonaceous meteorites. *Science* 379, eabn7850. https://doi.org/10.1126/science.abn7850

Yoshimura, T., Takano, Y., Naraoka, H., Koga, T., Araoka, D., *et al.* (2023) Chemical evolution of primordial salts and organic sulfur molecules in the asteroid 162173 Ryugu. *Nature Communications* 14, 5284. https://doi.org/10.1038/s41467-023-40871-0